Suitability of PVDF films for use in pressure-gradient acoustic intensity vector probes

Damien Killeen (1,2), David Matthews (1,2) and Andrew Munyard (1)

(1) Maritime Operations Division, DSTO, HMAS Stirling, Western Australia.
(2) Department of Applied Physics, Curtin University, Western Australia.

ABSTRACT

Pressure gradient vector probes are adversely affected by diffraction around internal components of the probe; however by constructing a pressure gradient probe from polyvinylidene difluoride (PVDF) sensor elements, which have acoustic impedance similar to seawater, the diffraction effects within the probe can be effectively minimised. For use in a pressure-gradient intensity vector probe though, the elements must be omni-directional. This paper discusses the design, construction and initial characterisation of a prototype two-dimensional pressure-gradient vector probe using four PVDF films as the sensing elements.

INTRODUCTION

Intensity is defined as energy flux density, in this context at a point in a wave field. In acoustics, it has long been established e.g. (Kinsler *et al.*, 1950) that the intensity vector is given by the product of the acoustic pressure and the fluid particle velocity vector induced by the acoustic disturbance:

$$\mathbf{I}_i(t) = p(t)\mathbf{u}_i(t) \tag{1}$$

Here $\mathbf{I}_i(t)$ is the instantaneous acoustic intensity vector at time t, $p(t)$ is the acoustic pressure and $\mathbf{u}_i(t)$ is the instantaneous fluid particle velocity vector.

Measurements of acoustic pressure are common-place in air and water, but fluid particle velocities on an acoustic scale are somewhat more problematic. In air acoustics, hot-wire anemometer techniques have enabled direct measurement of these velocities, but only relatively recently (de Bree *et al.*, 1996) and more recently also underwater (de Bree *et al.*, 2010). Underwater, neutrally buoyant sensors that can move with (and hence sense) fluid particle velocity have been demonstrated (Leslie *et al.*, 1956) and put to use. More recently, single-crystal accelerometers that have a very high sensitivity and very low noise floor (Wlodkowski *et al.*, 2001) have been used to produce much smaller vector intensity probes (Shipps *et al.*, 2003), but these are not available in Australia.

Air acousticians wanting to measure acoustic intensity prior to 1996 could not measure fluid particle velocity directly, so instead would measure the spatial gradient of pressure to estimate velocity. This estimate is based on the linear fluid momentum equation, that arises from the application of Newton's second law under uniform flow conditions e.g. (Kinsler *et al.*, 1950):

$$-\nabla p(t) \cong \rho \frac{\partial \mathbf{u}}{\partial t} \tag{2}$$

Here ∇ is the spatial gradient operator and ρ is fluid density.

If acoustic pressure is measured by two omni-directional sensors to give $p_1(t)$ and $p_2(t)$, and the sensors are separated by the vector $\mathbf{n}=(n\cos(\eta), n\sin(\eta))$, then $(p_1-p_2)/n$ is the finite difference approximation of the spatial gradient of pressure and $(p_1+p_2)/2$ estimates the pressure at the midpoint between the two sensors. Thus equation (1) can be estimated by:

$$I_\eta(t) \cong \frac{p_1(t)+p_2(t)}{2\rho n}\int_{-\infty}^{t}\left[p_1(\tau)-p_2(\tau)\right]d\tau \tag{3}$$

Here $I_\eta(t)$ is the component of the instantaneous acoustic intensity vector in the direction η.

Both the direct-measurement and pressure-gradient methods have associated challenges. Inertial measurement of velocity requires compliant mounting, calibration of the transfer function between fluid particle motion and probe motion, calibration of two different types of transducer, and requires less accessible sensor technology. Pressure-gradient probes are affected by sensor phase mismatch in all acoustic fields, as opposed to inertial sensors that are only affected in highly reactive fields (Jacobsen *et al.*, 2005). Pressure-gradient probes also introduce finite difference approximation errors.

It has also been shown that sound intensity estimates made with pressure-gradient probes are adversely affected by diffraction around sensing elements, pre-amplifier housing bodies and nearby mounting arrangements (Krishnappa, 1984). In air acoustics this has been used to offset finite difference approximation errors to almost double the effective frequency range of the probe (Jacobsen *et al.*, 1998) however this has not yet been replicated in underwater acoustics.

Diffraction effects can be reduced by moving impedance mismatched materials away from the acoustic centre of the probe (Krishnappa, 1983), and by reducing the impedance mismatch of probe components that cannot be moved away, such as the sensing elements.

The acoustic impedance of seawater is around 1.5 MNsm^{-3} whereas piezoelectric ceramic (PZT) acoustic impedance is around 20 times higher (Moffet *et al.*, 1986). In comparison, the acoustic impedance of PVDF is 2.7 MNsm^{-3} (*Piezo Film Sensors Technical Manual*, 2003); an order of magnitude better matched to seawater than PZT. Hence it is proposed that a pressure-gradient acoustic intensity probe made from PVDF sensing elements potted within an acoustically trans-

parent waterproofing compound will produce a more accurate intensity probe than one made with ceramic sensors.

If the pressure signals p_1 and p_2 of equation (3) are dependant on azimuth (θ_1 and θ_2), cross terms appear that require prior knowledge of θ_j to determine the intensity vector, vastly diminishing the utility of the probe. Hence, omni-directionality is crucial for pressure-gradient probe sensing elements.

The horizontal ($\phi=\pi/2$) directionality of a planar element such as a PVDF film can be modelled as a rectangular piston source (Urban, 2002):

$$\Gamma(\theta)\big|_{\phi=\pi/2} = \frac{\sin\left(ka\sin(\theta)/2\right)}{ka\sin(\theta)/2} \quad (4)$$

Here a is the width of the PVDF film, k is the wave number and θ is the azimuth. According to equation (4) for a film width a = 13 mm, the response is omni-directional within ±0.1 dB below 12 kHz, suggesting that such a film is suitable for use in a pressure-gradient intensity probe below this frequency. The directionality of voided PVDF film (perfectly impedance matched to water) potted within "a polyurethane known to be a good acoustic match to water" was measured at 100 kHz and confirmed equation (4) (Moffet *et al.*, 1986).

This paper details the characterisation of a prototype 2D intensity vector probe using PVDF elements for underwater use, and extends from previous work (Killeen *et al.*, 2009) by the addition of the second dimension and removal of a solid mounting piece internal to the probe which caused significant diffraction issues. PVDF pressure-gradient intensity probes have been considered in the past (Segota, 1990) as has a PVDF bimorph as a direct measure of fluid particle velocity (Josserand *et al.*, 1985).

APPARATUS

The pressure-gradient intensity probe was constructed by machining a block of Robnor polyurethane into a cuboid 18 mm by 18 mm by 45 mm and fixing to each side a 13 mm wide, 30 mm high, 56 µm thick doubled-over (for electromagnetic shielding) PVDF film. The sensing elements were then encased in a cylindrical outer layer of Robnor polyurethane of 30 mm diameter capped by an air filled PVC pipe that provided a waterproof path for the cables to exit the tank. Images of three stages of construction and an x-ray of the completed probe are shown in Figure 1.

The probe was placed in a rotational mount 0.50 m below the surface and 0.445 m from the centre of a freshwater tank of dimensions 1.0 m deep and 1.8 m diameter, as shown in Figure 2. An ITC1032 sound source was located at the centre of the tank, also 0.50 m below the surface. A calibrated Reson TC4014-5 reference hydrophone was diametrically opposed to the probe at the same depth. This arrangement produced a path length difference between the direct path and both the surface and bottom reflected paths of 0.65 m. By assuming a sound speed of 1500 ms^{-1} this equates to a delay of 0.43 ms between direct and reflected paths.

The ITC1032 was driven by an Agilent 33220A signal generator amplified by both stages of an Agilent 33502A two-stage 5-times voltage amplifier, providing 25-times voltage gain.

The probe's four sensors were connected to Krohn-Hite 3364 pre-amplifier units configured with 40 dB input gain, a 1 kHz high-pass filter and a 200 kHz low-pass filter (both 4-pole Butterworth). The Reson TC4014-5 includes 26 dB of pre-amplification, 6 dB of which was lost in the conversion from double- to single-ended signal. A Reson VP2000 (EC6081) voltage pre-amplifier with a 1 kHz to 250 kHz band-pass filter (and 0 dB gain) was applied to the TC4014-5 channel.

Three of the four probe channels and the TC4014-5 channel were monitored using a four channel Agilent DSO1024A 200 MHz oscilloscope as well as being recorded on a 4-channel Roland R4-Pro unit set to 24-bit precision and 96 kHz sample rate. All four recording channels were calibrated using a Neutrik signal generator providing white noise of 20 kHz bandwidth and -34 dBV RMS level.

RESULTS

Time-Gated Narrowband Pulse at 40 kHz

Ten wavelengths of a 40 kHz frequency pulse (0.25 ms pulse length) were transmitted every second though the ITC1032 transducer. The oscilloscope was used to measure RMS voltage levels in the stable section of each pulse received on the three probe channels under test and the TC4014-5 channel. The probe was then rotated by 10° increments through 360°. These pulses were also recorded for further analysis.

The directionality of the ITC1032 was also measured by rotating it and monitoring the voltage levels from the TC4014-5 on the oscilloscope. The source was found to be omni-directional within ±0.5 dB at 40 kHz.

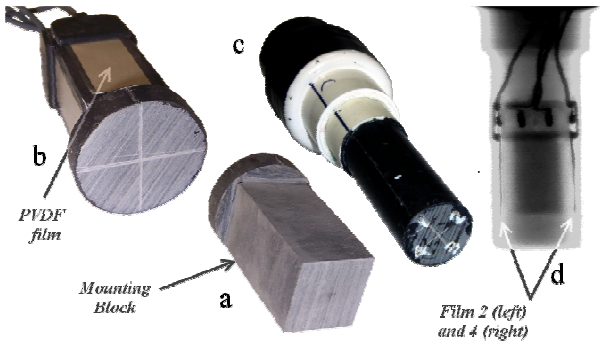

Figure 1. Robnor sensor mount (a) with PVDF films (b) outer Robnor layer (c) and x-ray imagery (d).

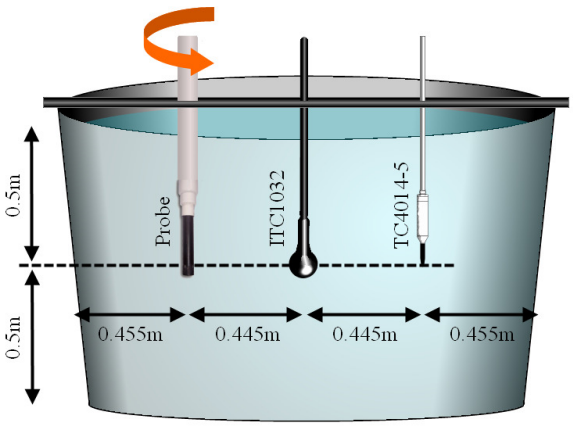

Figure 2. Experimental Setup.

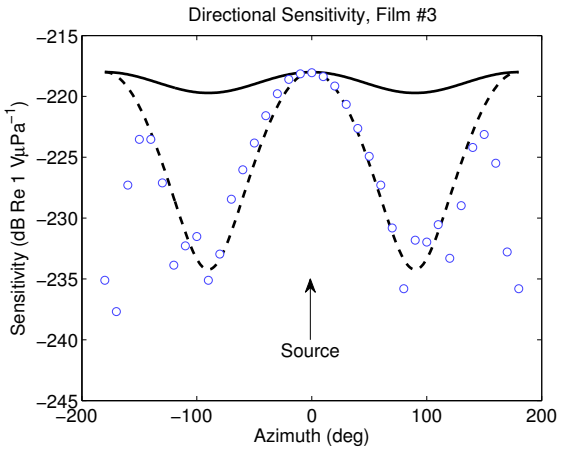

Figure 3. Film #3's directional sensitivity measured by time-gated 40 kHz pulses (circles) compared with equation (4) (solid line). A "best-fit" of equation (4) with a=33 mm is also shown (dashed).

Figure 3 shows the sensitivity of film #3 computed from the voltage amplitudes read off the oscilloscope screen for the time-gated narrowband pulse transmitted by the ITC1032. The other two films that were recorded show similar results but are excluded from the plot for clarity. Equation (4) is plotted for comparison as a solid line.

It is clear that equation (4) is not appropriate for modelling this film at 40 kHz. The null depth is only matched by increasing the width parameter a to an effective width of 33 mm, as shown by the dashed line in Figure 3. This may be due to the mismatch (however slight) between the acoustic impedance of the film to that of the polyurethane and the water. Even with this effective width "correction" there is a 20 dB loss at ±180° that equation (4) can not model. Losses such as these have been linked (Nakamura *et al.*, 1993) to the interaction between the incident, reflected and surface waves – the latter primarily associated with the backing (or in our case, encapsulating) material.

It is evident that lower frequency measurements of the film directionality are required to determine its omni-directionality rather than relying on modelled directivity patterns.

Time-gated Broadband Pulse

Traditional single frequency time-gate techniques in a tank of this size are limited to frequencies above around 30 kHz. This is due to the need for many (>10) cycles to produce a stable section in the middle of the received pulse that is not distorted by the impulse response of the receiver. These cycles, and the ramp down time associated with the transmitter and receiver impulse responses, need to total less time than the delay between the direct path arrival and that of the first multi-path.

It is also possible to transmit a broadband pulse, short enough to avoid multipath interference, but long enough for Fourier analysis of the received pulses to be useful. Each Fourier coefficient is analogous to the application of a filter whose frequency response is the Fourier transform of the time-gate window applied to the data, centred on the frequency bin. This has the effect of filtering out the distortion caused by ramp up and ramp down, so that the full pulse length is effectively "stable", if the frequency bin has a sufficient signal to noise ratio.

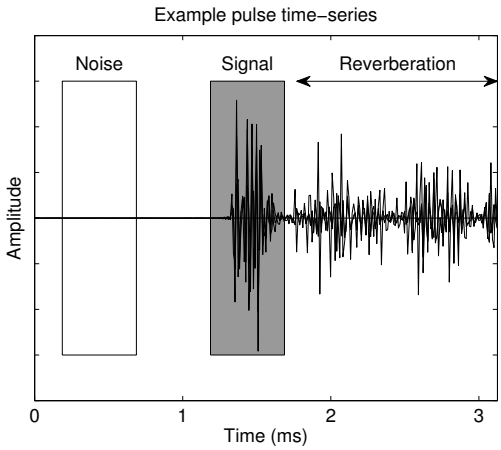

Figure 4. The selected regions of signal and noise for an example pulse.

A broadband pulse was created by generating 16,384 samples of Gaussian distributed white noise. A 12 kHz low-pass filter was applied to partially offset the transfer function of the ITC1032, followed by a Hanning window. The signal generator's DAC converted this pulse to a 0.25 ms long continuous voltage, output once per second. At least 30 identical pulses were recorded by the R4-Pro before rotating the probe by 10°. This was repeated to cover the full 360°.

A 0.5 ms section of data (48 samples) was selected around each broadband pulse such that the last sample corresponded to the lowest point in between the direct and reflected signals (see Figure 4). This allowed for the most relaxation time possible without any multipath interference. These samples were then passed through Matlab's discrete Fourier transform (FFT).

For comparison 48 samples of noise-only data, beginning 1 ms (96 samples) before the first sample used for each pulse (see Figure 4), were also processed in the same manner. By using this data immediately preceding each pulse the greatest possible relaxation time for the tank was achieved. The spectral content of the pulses received on the TC4014-5 is shown in Figure 5, and compared to the background noise spectra.

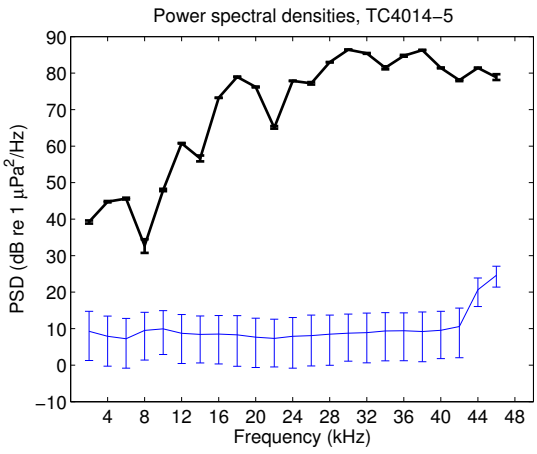

Figure 5. Median spectra of the broadband pulse received by the TC4014-5 (thick line), compared with background noise spectra (thin line). Error bars indicate 10th-90th percentiles.

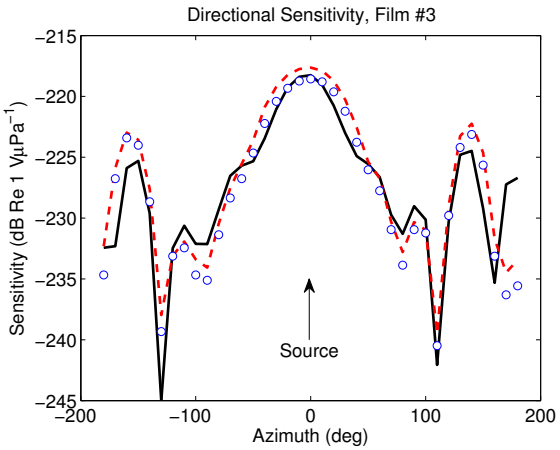

Figure 6. Comparison of sensitivity measurement techniques at 40 kHz: narrowband pulse oscilloscope (circles); Narrowband pulse DFT (solid); and broadband pulse DFT (dashed).

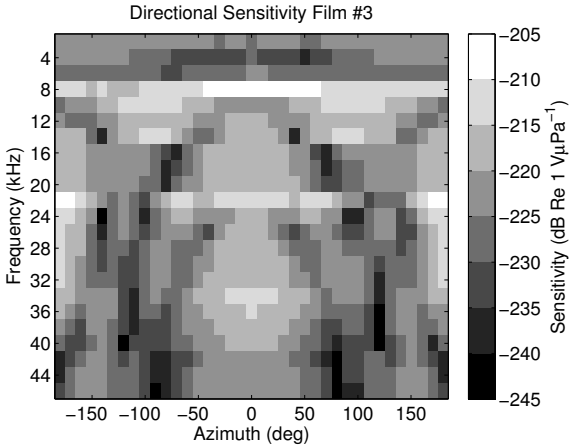

Figure 7. Intensity plot of the broadband measurement of spectral and directional sensitivity.

For each frequency bin the median value of all of the pulses' spectra collected at each angle was bandwidth corrected, and converted to a mean-square voltage using the calibration data recorded on each channel from the Neutrik voltage source. The calibration curve supplied with the TC4014-5 was then used to convert the TC4014-5 channel's voltage levels into pressure. Within the limits of the measured directionality of the ITC1032 (±0.5 dB), it was assumed that the pressure incident on the probe's sensor channels was identical to that on the TC4014-5, and thus the probe's sensors' directional sensitivity was determined.

The results of this method in the 40 kHz bin for both the narrowband and broadband pulses are compared in Figure 6 to the oscilloscope results of the previous section. There is general agreement between the methods at this frequency, except for the broadband pulse result around 180°.

The directional sensitivity measured in each frequency bin is shown in Figure 7. Clear, symmetric lobal structure is observed as low as 10 kHz, though it should be noted that at this frequency the pulse length is only 2.5 cycles.

These results need to be confirmed by comparison with the narrowband method of the previous section, in a larger tank where lower frequencies can be examined. This is further work, but other properties of the data presented here can be used to lend it more credibility.

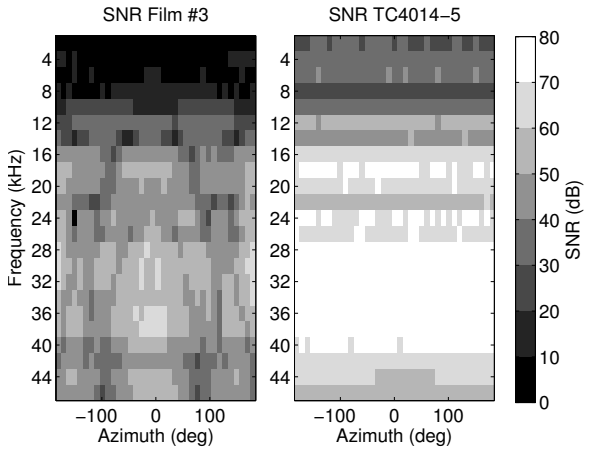

Figure 8. Median SNR values for the BB measurements for PVDF film #3 (left) and the TC4014-5 (right).

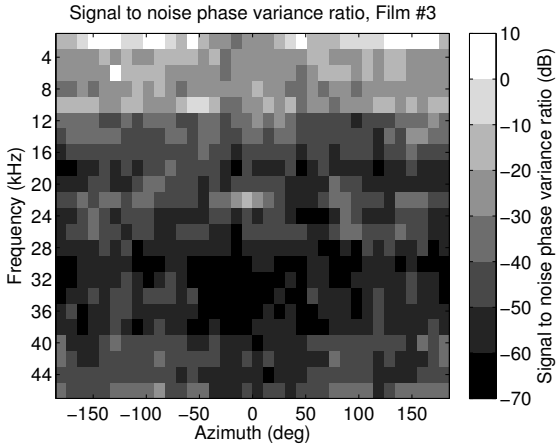

Figure 9. Ratio of signal phase-difference variance to noise phase-difference variance (0 dB indicates signal phase is as variable as the noise only case).

As mentioned previously, for each pulse processed, an identical length of data just prior to the pulse's arrival was also processed to capture the noise only level. The signal to noise ratio (SNR) of each pulse in each frequency bin was computed as the ratio of the pulse's spectrum to that of the noise immediately preceding it. The median SNR values across all the pulses recorded at each azimuth is plotted in Figure 8 for PVDF film #3 and the TC4014-5. The SNR is greater than 10 dB for frequencies 10 kHz and over on the PVDF channel, and does not fall below 20 dB on the TC4014-5.

Another indicator of data quality is the stability of the phase difference between the PVDF channels and the TC4014-5. At each azimuth, over 30 identical pulses are transmitted while the equipment is motionless. For frequency bins dominated by pressure signals from the ITC1032, the difference in phase between any PVDF channel and the TC4014-5 will remain constant over all pulses. The phase differences for a bin that is corrupted by noise at either the PVDF sensor or the TC4014-5 (or both) will fluctuate randomly. This fluctuation will be bounded (roughly) by the phase difference fluctuation observed in the noise-only sections.

The phase angle of each Fourier coefficient for each pulse received by the PVDF channels was compared to that of the TC4014-5 channel. The variance of this phase angle difference (after treatment for wrap-around through ±360°) was

then divided by the variance of the same phase angle differences computed for the noise-only sections preceding each pulse. The ratio of signal phase difference variance to noise phase difference variance (SPVNR) is shown in Figure 9. The ratio exceeds -20 dB below 12 kHz, suggesting that these frequencies are at least partially noise corrupted.

CONCLUSION

A pressure-gradient intensity probe made from materials that closely match the acoustic impedance of seawater will produce greater accuracy than one made from stiff materials such as PZT ceramics. PVDF film has already been used to make an acoustically transparent hydrophone (Moffet *et al.*, 1986) however omni-directionality of the films must be demonstrated before they can be used in a pressure-gradient acoustic intensity probe.

A prototype 2D pressure-gradient acoustic-intensity vector probe has been constructed using PVDF films. The directionality of these films was measured at high frequencies (40 kHz) and found to be more directional than expected.

A Fourier analysis technique was proposed and used to measure the directionality of the films at much lower frequencies than would normally be considered in a small tank. Whilst the results have not yet been confirmed with conventional time-gated single frequency techniques in a larger tank, it has been shown that the SNR and phase consistency indicate the results to be meaningful down to 10 kHz, three times lower than the usual rules of thumb for time-gate pulse measurements in a tank this size.

The accuracy of the method needs to be confirmed by time-gated pulsing of lower frequencies in a much larger tank. If the accuracy of the technique is confirmed, it can be used in the larger tank to test for omni-directionality of the films at frequencies below 10 kHz.

ACKNOWLEDGEMENTS

This work has been undertaken as part of the primary author's PhD study at Curtin University, supported by DSTO. The authors would like to thank Dr Alec Duncan, one of the PhD supervisors, for insightful discussion and simulation code.

REFERENCES

de Bree, H.-E., Leussink, P., Korthorst, T., Jansen, H., Lammerink, T. S. J. & Elwenspoek, M. 1996, 'The [mu]-flown: a novel device for measuring acoustic flows', *Sensors and Actuators A: Physical*, vol. 54, no. 1-3, pp. 552-557

de Bree, H.-E., Tjis, E. & Akal, T. 2010, 'The Hydroflown: MEMS-Based Underwater Acoustical Particle Velocity Sensor. Results of lab tests and sea trials.', *ECUA 2012*, Istanbul, pp 1-4

Jacobsen, F., Cutanda, V. & Juhl, P. M. 1998, 'A numerical and experimental investigation of the performance of sound intensity probes at high frequencies', *The Journal of the Acoustical Society of America*, vol. 103, no. 2, pp. 953-961

Jacobsen, F. & de Bree, H.-E. 2005, 'A comparison of two different sound intensity measurement principles', *The Journal of the Acoustical Society of America*, vol. 118, no. 3, pp. 1510-1517

Josserand, M. A. & Maerfeld, C. 1985, 'PVF2 velocity hydrophones', *The Journal of the Acoustical Society of America*, vol. 78, no. 3, pp. 861-867

Killeen, D., Legg, M. & Matthews, D. 2009, 'A prototype PVDF underwater pressure-gradient acoustic intensity probe', *Proceedings of Acoustics 2009*, Australian Acoustical Society, Adelaide, pp 1-6

Kinsler, L. E., Frey, A. R., Coppens, A. B. & Sanders, J. V. 1950, *Fundamentals of Acoustics*, John Wiley & Sons, Inc, New York

Krishnappa, G. 1983, 'Interference Effects in the Two Microphone Technique of Acoustic Intensity Measurements', *Noise Control Engineering Journal*, vol. 21, no. 3, pp. 126-135

Krishnappa, G. 1984, 'Scattering/Diffraction Effects in the Two-Microphone Technique of Measuring Sound Intensity at Sound Incidence Angles Other than 0 degrees', *Noise Control Engineering Journal*, vol. 22, no. 3, pp. 96-102

Leslie, C. B., Kendall, J. M. & Jones, J. L. 1956, 'Hydrophone for Measuring Particle Velocity', *The Journal of the Acoustical Society of America*, vol. 28, no. 4, pp. 711-715

Moffet, M. B., Powers, J. M. & McGrath, J. C. 1986, 'A ρc hydrophone', *Journal of the Acoustic Society of America*, vol. 80, no. 2, pp. 375-382

Nakamura, Y. & Otani, T. 1993, 'Study of surface elastic wave induced on backing material and diffracted field of a piezoelectric polymer film hydrophone', *The Journal of the Acoustical Society of America*, vol. 94, no. 3, pp. 1191-1199

Piezo Film Sensors Technical Manual, 2003, Measurement Specialties, Inc. Sensor Products Division, Hampton

Segota, J. P. 1990, *The design, construction, and evaluation of a two-hydrophone intensity probe to determine the feasibility and limitations of underwater intensity, energy density, and impedance measurements*, The Pennsylvania State University,

Shipps, J. C. & Deng, K. 2003, 'A miniature vector sensor for line array applications', *OCEANS 2003. Proceedings*, pp 2367-2370 Vol.5

Urban, H. G. 2002, 'Rectangular Piston Source', *Handbook of Underwater Acoustic Engineering*, STN ATLAS Elektronik GmbH, Bremen, 8.2.7, pp 185

Wlodkowski, P. A., Deng, K. & Kahn, M. 2001, 'The development of high-sensitivity, low-noise accelerometers utilizing single crystal piezoelectric materials', *Sensors and Actuators A: Physical*, vol. 90, no. 1-2, pp. 125-131